

Umbilical Cord-Derived Mesenchymal Stem Cell-Derived Exosomes Combined Pluronic F127 Hydrogel Promote Chronic Diabetic Wound Healing and Complete Skin Regeneration

This article was published in the following Dove Press journal:
International Journal of Nanomedicine

Jiayi Yang^{1,*}
Zhiyi Chen^{1,*}
Daoyan Pan^{1,*}
Huaizhi Li¹
Jie Shen^{1,2}

¹Department of Endocrinology and Metabolism, The Third Affiliated Hospital of Southern Medical University, Guangzhou, People's Republic of China; ²Shunde Hospital of Southern Medical University, Shunde, People's Republic of China

*These authors contributed equally to this work

Purpose: Chronic refractory wounds are a multifactorial comorbidity of diabetes mellitus with the characteristic of impaired vascular networks. Currently, there is a lack of effective treatments for such wounds. Various types of mesenchymal stem cell-derived exosomes (MSC-exos) have been shown to exert multiple therapeutic effects on skin regeneration. We aimed to determine whether a constructed combination of human umbilical cord MSC (hUCMSC)-derived exosomes (hUCMSC-exos) and Pluronic F-127 (PF-127) hydrogel could improve wound healing.

Materials and Methods: We topically applied human umbilical cord-derived MSC (hUCMSC)-derived exosomes (hUCMSC-exos) encapsulated in a thermosensitive PF-127 hydrogel to a full-thickness cutaneous wound in a streptozotocin-induced diabetic rat model. The material properties and wound healing ability of the hydrogel and cellular responses were analyzed.

Results: Compared with hUCMSC-exos, PF-127-only or control treatment, the combination of PF-127 and hUCMSC-exos resulted in a significantly accelerated wound closure rate, increased expression of CD31 and Ki67, enhanced regeneration of granulation tissue and upregulated expression of vascular endothelial growth factor (VEGF) and factor transforming growth factor beta-1 (TGF β -1).

Conclusion: The efficient delivery of hUCMSC-exos in PF-127 gel and improved exosome ability could promote diabetic wound healing. Thus, this biomaterial-based exosome therapy may represent a new therapeutic approach for cutaneous regeneration of chronic wounds.

Keywords: angiogenesis, diabetes wound, exosomes, mesenchymal stem cells, thermoresponsive hydrogels

Introduction

Diabetes mellitus is a chronic disease worldwide. According to an epidemiological survey released by the World Health Organization, the global prevalence of diabetes among adults (20–79 years) will increase from 6.4% in 2010 to 7.7% in 2030, which means that the number of affected adults will increase from 285 million to 439 million.¹ Hyperglycemia-induced vascular damage may be one of the major factors leading to severe diabetic complications, including diabetic foot ulcers (DFUs).² It has been reported that 10–25% of individuals with diabetes suffer from DFUs,³ which place a great burden on patients and medical institutions.⁴

Correspondence: Jie Shen; Daoyan Pan
Department of Endocrinology and Metabolism, The Third Affiliated Hospital of Southern Medical University, Guangzhou 510515, People's Republic of China
Email shenjiedr@163.com; pdy4266@126.com

Although current conventional treatments for DFUs, including debridement, wound dressing, lesion pressure reduction, anti-infection measures, peripheral vascular lesion management and strict blood glucose control,⁵ is relatively mature and new treatments are being developed, the DFUs treatment outcomes are still not satisfactory.⁶ DFU-associated amputations have been estimated to accounted for 84% of all diabetes-related lower limb amputations and can lead to severe depression and death and bring out great social burden.^{7,8} Therefore, the development of more effective treatments for DFUs has become a critical clinical challenge.

In recent years, mesenchymal stem cells (MSCs) have been shown to play important roles in tissue regeneration and wound repair through accelerating wound closure,^{9,10} enhancing re-epithelialization,¹¹ increasing angiogenesis,^{12–14} modulating inflammation,¹⁵ and regulating ECM remodeling.¹⁰ In previous studies on wound healing, cells have been injected locally into or around the wound area, and the treatment effects have been limited by the non-optimal retention of the cellular therapy.¹⁶ In addition, a study revealed that the diabetic-wound micro-environment is not conducive to the survival, proliferation and differentiation of stem cells, and that the survival time of exogenous stem cells in diabetic wounds is relatively short.¹⁷ Recent studies have found that extracellular vesicles (EVs), which are 40–5000-nm particles released by cells and includes exosomes, microvesicles and apoptotic bodies, can effectively regulate long- or short-distance intercellular communication through their various bioactive cargos, including DNA, RNA, microRNA (miRNA) and protein.¹⁸ It is currently believed that MSC-exos have a tissue-repair ability equal to or greater than that of MSCs themselves. More importantly, compared with cell transplantation, EV-mediated cell-free therapies offer the advantages of greater stability and storability, no risk of ectopic tissue formation and having a lower possibility of immune rejection.¹⁹ Recent studies have also shown that MSC-exos have the potential to promote wound repair. Exosomes derived from human umbilical cord MSCs (hUCMSCs) have been reported to exerts proangiogenic effects and thereby accelerated cutaneous wound healing.²⁰ Furthermore, a study confirmed that exosomes derived from induced pluripotent stem cells-derived MSCs promote cutaneous wound healing by promoting collagen synthesis and angiogenesis.²¹ However, there are challenges in the application of exosomes to treat wounds because exosomes are rapidly cleared from the application site and survive *in vivo* for only a short time.¹³ Therefore, the combination of exosomes with biomaterials that extend the retention time of exosomes on the

wound surface without affecting their biological activity has become a focus of research to develop exosome-based therapies.

Many studies have shown that hydrogels can enhance cell properties and processes, such as cell growth rate, bone formation, and vascular anastomosis, etc. Hydrogels can also encapsulate cells, form scaffolds and act as drug carriers.¹³ A study of the repair of joint damage via exosomes showed that²² exosomes carried in a chitosan hydrogel showed a decreased degradation rate. Subsequent research has revealed that exosomes can be delivered to injury sites by a variety of carriers. Shi et al²³ used a biodegradable and biocompatible chitosan/silk hydrogel sponge to deliver the human gingival MSC-derived exosomes to diabetic wound tissue of rats and reported that the compounds could promote wound healing through re-epithelialization, collagen deposition and angiogenesis. Another study reported that chitosan hydrogel combined with exosomes derived from human placenta-derived MSCs (hPMSCs) was able to increase the stability of proteins and microRNAs in exosomes and was superior to exosomes alone for treating a hind limb ischemic model.²⁴ In addition, a photoinduced imine crosslinking hydrogel glue was found beneficial for retaining stem cell-derived exosomes, and the combination promoted the repair and regeneration of articular bone defects.¹³ Although there are studies showing the beneficial effects of exosome-loaded hydrogels applied to a variety of injury sites, few studies have investigated the treatment effects of combinations of hUCMSC-derived exosomes (hUCMSC-exos) and biomaterials, such as hydrogels, on chronic wounds, especially diabetic wounds.

Therefore, we aimed to explore the ability of a wound-friendly hydrogel that can carry hUCMSC-exos to promote wound healing. Pluronic F-127 (PF-127, also known as Poloxamer 407) has unique heat-sensitive properties: it exists as a liquid at low temperature and as a semisolid gel at high temperature. Due to this reversible thermoresponsive behavior, PF-127 can fit into the complex and irregular space of diabetic foot wounds, allowing the bioactive agent to adhere to the target sites and exert its biological effects.²⁵ Previous studies reported that PF-127 has a porous structure, which can prolong the release time of therapeutic proteins and increase the drug half-life in serum.²⁶ Due to these characteristics of PF-127, we hypothesized that the PF-127 can retain and sustainedly release hUCMSC-exos directly onto injured tissues, for which can attract fibroblasts and endothelial cells, benefitting wound repair.²⁷

Furthermore, PF-127 has a mild inflammatory property and the ability to absorb the secretions from the wound surface, maintaining a moist, adequate healing environment.²⁸ Moreover, the topical application of a combination of hUCMSC-exos and PF-127 is a simple and non-invasive treatment and may be regarded as a high-efficiency, low-toxicity delivery method.

Here, we aimed to improve wound healing in a diabetic rat model by externally applying a constructed combination of hUCMSC-exos and PF-127 hydrogel. We investigated whether the exosome-hydrogel combination could better accelerate the wound healing rate in the diabetic rat model. Furthermore, we observed angiogenesis, cell proliferation, granulation tissue formation and other wound site phenomena to identify the wound repair mechanism of the exosome-hydrogel composites.

Materials and Methods

hUCMSC and HUVEC Culture

The hUCMSC line Saliat-HMSC(UC)-N was obtained from Guangzhou Saliat Stemcell Co., Ltd. The cells were tested for bacteria, fungi, mycoplasma and virus contamination and were shown to express a variety of stem cell-specific markers and to have good potential for proliferation and differentiation. The hUCMSC cell line was cultured in DMEM/F12 (Gibco, USA) containing 10% exosome-free serum (Gibco, USA) and 1% penicillin-streptomycin solution (Gibco, USA). The human umbilical vein endothelial cell (HUVEC) line c-12,206 (PromoCell, Germany), a single donor cell line, was procured and tested for bacteria, fungi, mycoplasma and virus contamination. These cells were cultured in MEM-alpha (Gibco, USA) containing 10% fetal bovine serum (Gibco, USA) and 1% penicillin-streptomycin solution (Gibco, USA).

Exosome Extraction and Identification

Exosomes were extracted using an exosome extraction kit. First, the supernatant of P3-P5 hUCMSCs was collected, and ExoQuick-TC (SBI, USA) exosome extraction reagent was added to the supernatant at a ratio of 1:5. After incubation overnight (>12 h) at 4°C, the supernatant was discarded, and the mixture was centrifuged at 1500 xg for 5 min to remove all liquid. Finally, 100–500 µL PBS was used to resuspend the obtained exosomes. A BCA quantitation kit (Beyotime, Shanghai, China) was used to determine the protein content of the exosome suspension. hUCMSC-exos were used for experiments or stored at

–80°C. hUCMSC-exos were analyzed for morphology, size, and marker (CD63 and CD81) expression by conventional transmission electron microscopy, NanoSight, and Western blotting, respectively.

Exosome-Hydrogel Composite Construction and Temperature Sensitivity Determination

According to the protein concentration of the hUCMSC-exos measured as described above, the exosome suspension was diluted with the appropriate volume of PBS to the target concentration of 300 µg/mL and then cooled in a 4°C refrigerator for 2 h. Precooled PF-127 powder (Sigma, USA) and 300 µg/mL hUCMSC-exos suspension were mixed in a 1.5 mL Eppendorf tube in an ice bath and then stored in a 4°C refrigerator. Eppendorf tubes were checked for precipitates after 1 h; if a precipitate was present, the mixture was blended and stored at 4°C; this process was repeated until the precipitate was completely dissolved. Finally, we obtained the hUCMSC-exos and PF-127 composite (hUCMSC-exos/PF-127). We adjusted the water bath temperature to 10°C and tested the initial gelation temperature of the hUCMSC-exos/PF-127 solution at different concentrations (20%, 22%, 24%, 26%, and 28%) over the temperature range of 10–40°C. Another constant temperature water bath was adjusted to 37°C, and the specific gelatinization time at 37°C was determined using a concentration gradient of hUCMSC-exos/PF-127.

Uptake of hUCMSC-Exos

Exosomes were labeled with the PKH67 kit according to the manufacturer's instructions (Sigma, USA) and stored at 4°C for later use. The prepared 24% PF-127 hydrogel was mixed with labeled exosomes in an ice bath until the precipitate had completely dissolved, and the resulting mixture was stored at 4°C. HUVECs seeded in 12-well plates were divided into four groups: 1) hUCMSC-exos/PF-127 group: 1 mL hUCMSC-exos/PF-127; 2) hUCMSC-exos group: 1 mL hUCMSC-exos; 3) PF-127 hydrogel group: 1 mL 24% PF-127; and 4) Control group: 1 mL PBS. Cells were incubated in an incubator with 5% CO₂ in the dark for 12 h. A 1:1000 DAPI nuclear staining solution was prepared with PBS. The cells were placed on ice, washed three times with PBS and then incubated in the dark for 30 min with the diluted DAPI stain. Four different fields of view in each group were randomly imaged with a light microscope (Leica®, Germany), and statistical analysis was conducted.

Migration and Proliferation Assays

Cell migration was assessed using a scratch assay. HUVECs were seeded in 6-well plates at a density of 1.2×10^5 cells/mL and cultured to 100% confluence. Four groups were analyzed: 1) hUCMSC-exos group: 3 mL hUCMSC-exos; 2) hUCMSC supernatant group: 3 mL hUCMSC supernatant; 3) PF-127 hydrogel group: 1 mL 24% PF-127 with DMEM (Gibco, USA); and 4) Control group: 1 mL DMEM. Five parallel scratches were made in each well with a 200 μ L pipette tip, and the width of each scratch was measured as the baseline value. The cells were then cultured with different reagents in a 5% CO₂ incubator for 0, 4, 8, 12, 18 and 24 h. The width of the scratch was visualized with a light microscope (Leica®, Germany) and measured by mimicking an exclusion zone assay using ImageJ software. For the proliferation assay, we used a transwell system (8- μ m pore size; Corning, USA) to evaluate the effect of hUCMSC-exos/PF-127 on HUVEC proliferation. Three groups were analyzed: 1) hUCMSC-exos/PF-127 group: 1 mL hUCMSC-exos/PF-127; 2) hUCMSC-exos group: 1 mL hUCMSC-exos; and 3) Control group: 1 mL DMEM. HUVECs (1×10^5 cells/well) were placed in the lower chamber of the transwell system, and the other three intervention substances were added to the upper chamber. CCK-8 reagent (Dojindo, Japan) was added to the medium on days 1, 2, 3, 4 and 5 after inoculation, and the results were analyzed after incubating the plates at 37°C for 1 h.

Diabetic Rat Model

Sprague-Dawley (SD) rats (male, 210±25 g, aged approximately 10 weeks) were provided by the SPF Animal Experimental Center of Southern Medical University (Guangzhou, China). All rats were fed in a room with a 12-h light/dark cycle and stable temperature (25°C) and humidity. Streptozotocin (STZ, 50 mg/kg, Sigma, USA) was dissolved in citrate-sodium citrate buffer (pH 4.4) to obtain a 1% STZ solution, which was then intraperitoneally injected into SD rats fasted for 18 h to generate a model of diabetes. Blood glucose levels in the rats were measured on days 3, 7, 10 and 14 after induction using Accu-Chek Advantage strips (Roche, Germany). The rats with blood glucose levels above 16.67 mmol/L one week after injection were diagnosed with diabetes. After the 3 weeks of diabetic state after STZ injection, a wound healing model was created. The importation, transportation, housing, and breeding of the rats were all conducted according to the recommendations of “The use

of nonhuman primates in research.” The rats were euthanized by cervical dislocation to prevent suffering. The Southern Medical University Animal Care and Use Committee approved all procedures involving rats.

Surgical Procedure

After 3 weeks of hyperglycemia induced by STZ injection, 24 diabetic rats were anesthetized by an intraperitoneal injection of Nembutal (35 mg/kg, Sigma, USA). After anesthesia was achieved, the dorsal skin was shaved and sterilized with 75% ethyl alcohol. Two symmetrical, circular, full-thickness skin wounds of 10 mm in diameter were made 1.5 cm apart. The 24 rats were randomly divided into two groups, and the wounds in each groups were randomly divided into four treatment groups: 1) hUCMSC-exos/PF-127 group: 100 μ g hUCMSC-exos dissolved in 100 μ L Pluronic F127 hydrogel (24%); 2) hUCMSC-exos group: 100 μ g hUCMSC-exos dissolved in 100 μ L PBS; 3) PF-127 hydrogel group: 100 μ L PF-127 hydrogel (24%); and 4) Control group: 100 μ L PBS. The four different materials were injected topically to cover the wound. Next, Tegaderm™ (3M, USA) was then applied to the wound area and was changed every 3 days. The post-operative rats were housed individually.

Analysis of Wound Closure Rate

The survival and wound healing conditions of each group were observed. The change in size of each diabetic wound was determined from photographs obtained on days 0, 3, 7, 10 and 14 after surgery and analyzed by ImageJ (NIH, USA). The wound closure rate was calculated to represent the size change in wound size from the original size using the formula Wound healing rate = $(S_0 - S_A) / S_0 \times 100\%$, where S_0 represents the original wound area on day 0, and S_A represents the wound area on day A.

Hematoxylin and Eosin (H&E) Staining

Full-thickness traumatic tissue samples of approximately 3 mm were harvested along the outer edge of the entire wound on day 14. All the tissues were divided into two equivalent pieces: one piece was fixed in 4% paraformaldehyde at 4°C overnight and then embedded in paraffin, and the other piece was stored in liquid nitrogen for reverse transcription-polymerase chain reaction (RT-PCR) gene expression analysis. Tissue sections (4 μ m) were fixed on glass slides for histological analysis. H&E staining was performed to visualize the pathological alterations in the tissue at different time points. Photographs were

taken at 5X and 10X magnification using a microscope and digital camera (Zeiss, Germany).

CD31 Immunohistochemistry and Quantitation of Microvessel Density

Immunohistochemistry of tissue sections with rabbit anti-rat CD31 antibody (Santa Cruz Biotechnology, USA) was performed at 7 and 14 days to detect angiogenesis in the wound after intervention. Sections were deparaffinized, rehydrated, heated in a microwave oven twice for antigen recovery, treated with 3% H₂O₂ and then incubated with 5% goat serum albumin. Then, the sections were incubated overnight at 4°C with primary rabbit anti-rat CD31 antibody (1:75, Santa Cruz Biotechnology), followed by a 1-h incubation with HRP-conjugated goat anti-rabbit secondary antibody (1:200, Abcam) and visualization with a DAB kit (ZSGB-BIO, China). After being counterstained with hematoxylin, the slides were assessed with a fluorescence microscope (40FL Axioskop, Zeiss).

The three regions with the most neovascularization at low magnification (5X) on each slide were selected. Then, three randomly selected areas in each region were imaged at 20X magnification. These images were analyzed with Image-Pro Plus software. The mean number of blood vessels per image was defined as the microvascular density (MVD).

Ki67 Immunofluorescence

To detect the effects of the four treatments on cell proliferation at the wound site, immunofluorescence of the wound sections was performed on day 7. After conventional dewaxing, hydration, antigen recovery, and blocking, the cells were incubated with rabbit anti-Ki67 primary antibody (1:800, Abcam, USA) and then with goat anti-rabbit IgG Alexa Fluor[®] 594-conjugated secondary antibody (1:400, Abcam, USA) and DAPI. The stained sections were imaged at 20X on a fluorescence microscope, and 5 randomly selected regions in each sample were analyzed. Then, Image-Pro Plus software was used to calculate the percentage of positive cells in each group.

RNA Preparation and RT-PCR Analysis

To explore the mechanism underlying the therapeutic effect, the mRNA expression levels of vascular endothelial growth factor (VEGF) and transforming growth factor beta-1 (TGFβ-1), two key growth factors considered to be associated with wound healing, were examined. Total RNA was extracted from full-thickness traumatic tissue using TRIzol

reagent (Keygen, China) according to the manufacturer's instructions. Next, the extracted total RNA was used to synthesize cDNA using the HiScript II Q RT SuperMix for qPCR kit. RT-PCR, using ChamQ SYBR qPCR Master Mix, cDNA and the primers described below, was performed on a Roche LightCycler[®]96 system, according to the manufacturers' instructions. The housekeeping gene β-actin was used to determine and normalize the relative expression level of each RNA sample. The standard 2^{-ΔΔCt} method was used for data analysis. The primer sequences were as follows:

βactin-F: 5'TGCTATGTTGCCCTAGACTTCG
 βactin-R: 5'GTTGGCATAGAGGTCTTTACGG
 VEGF-F: 5'CAATGATGAAGCCCTGGAGTG
 VEGF-R: 5'GCTCATCTCTCCTATGTGCTGG
 TGFβ1-F: 5'GGCGGTGCTCGCTTTGTA
 TGFβ1-R: 5'TCCCGAATGTCTGACGTATTGA

Statistical Analysis

Data are reported as the mean ± standard deviation. Differences among groups were evaluated by one-way analysis of variance (ANOVA) followed by Tukey's post-test (Graph Pad Prism 7.0), and 95% confidence intervals were calculated. Differences were considered statistically significant at *p < 0.05 and **p < 0.01.

Results

Exosome Characterization

Approximately 3 mL hUCMSC-exos at a concentration of 1617.2 μg/mL were obtained from 50 mL hUCMSC supernatant according to the BCA protein quantification kit. Transmission electron microscopy showed that hUCMSC-exos had a typical "saucer-like" exosome structure (Figure 1A). Samples of hUCMSC-exos were analyzed with a NanoSight LM 10; the concentration was determined to be 4.19×10¹¹ particles/mL, and 44.4% of the particles were within the size range of 30 nm to 150 nm (Figure 1B). CD63 and CD81 protein expression levels were significantly increased in hUCMSC-exos compared with hUCMSCs. (Figure 1C). These findings confirmed that exosomes can be successfully extracted from hUCMSC supernatant with the employed exosome extraction kit.

Temperature Sensitivity and Uptake of Exosome-Hydrogel Complexes

As the Pluronic F127 concentration increased, the initial gelling temperature (IGT) of hUCMSC-exos/PF-127

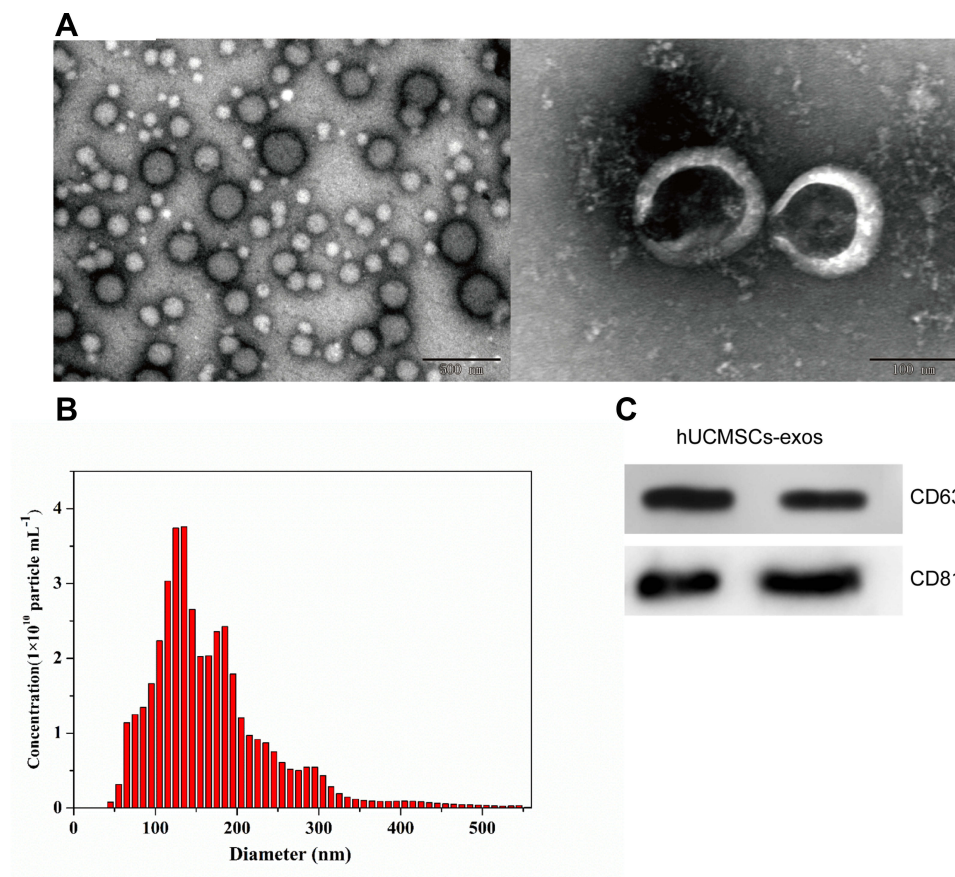


Figure 1 (A) Electron microscopy images of exosomes derived from human umbilical cord mesenchymal stem cell (hUCMSCs-exos). (B) Histogram of the diameter and concentration of hUCMSCs-exos determined by NanoSight. (C) Expression of CD63 and CD81 (exosomes markers) in hUCMSCs-exos determined by Western blotting.

decreased. The 20% hUCMSC-exos/PF-127 composite initially gelled at 17.8°C, while the 28% hUCMSC-exos/PF-127 composite gelled at 12.4°C. The gel formation time was inversely proportional to the temperature. The prepared 24% hUCMSC-exos/PF-127 mixture was liquid at 4°C and in a semisolidified colloidal state at 37°C (Table 1). After a 12-h incubation with different reagents, HUVECs showed green fluorescence representing hUCMSC-exos in the

Table 1 The Initial Gelling Temperature and 37°C Gelling Time of Gel Complex in Different Exosomes Concentration (Mean \pm sd)

| Concentration | Initial Gelling Temperature (IGT) °C | Gelling Time at 37°C |
|---------------|--------------------------------------|----------------------|
| 20% | 17.8 \pm 0.7 | 1min32s \pm 6s |
| 22% | 16.6 \pm 0.3 | 1min19s \pm 5s |
| 24% | 14.6 \pm 0.5 | 1min08s \pm 3s |
| 26% | 13.4 \pm 0.3 | 51s \pm 3s |
| 28% | 12.4 \pm 0.1 | 46s \pm 2s |

cytoplasm, with signal enrichment around the nucleus, while HUVECs cocultured with PBS and 24% PF12 did not show obvious green fluorescence. These data indicate that hUCMSC-exos can penetrate the cell membrane and concentrate around the nucleus (Figure 2).

hUCMSC-Exos/PF-127 Promote the Migration and Proliferation of HUVECs in vitro

As shown in Figure 3A and Figure 3B, the hUCMSC-exos and supernatant groups showed greater cell migration than the PF-127 hydrogel group and control group, and the hUCMSC-exos/PF-127 group exhibit the best performance, as confirmed by optical microscopy. The CCK-8 assays showed that hUCMSC-exos/PF-127 promoted HUVEC proliferation better than the other two treatments, confirming that the hydrogel prolongs exosome survival in vitro and maintains their biological activity (Figure 3C).

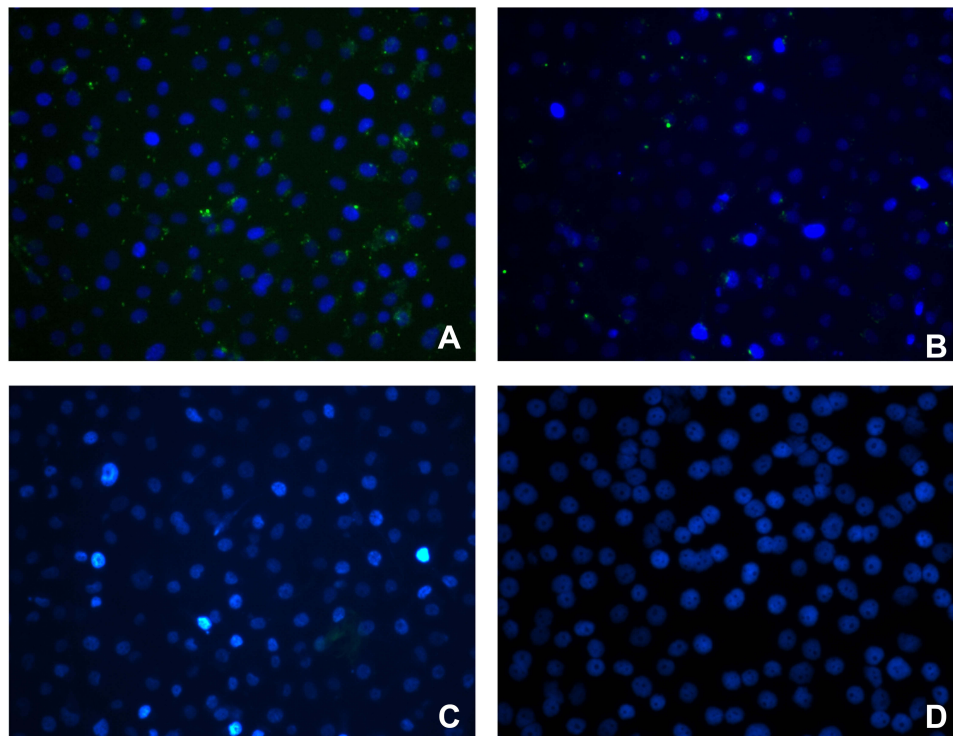


Figure 2 PKH67 staining to trace the cellular localization of exosomes. 400X magnification. Green, PKH67 (exosomes staining solution); blue, DAPI (nucleus staining solution). (A) hUCMSCs-exos/PF-127: exosomes combined with PF-127, (B) exosomes, (C) PF-127, (D) PBS (phosphate-buffered saline).

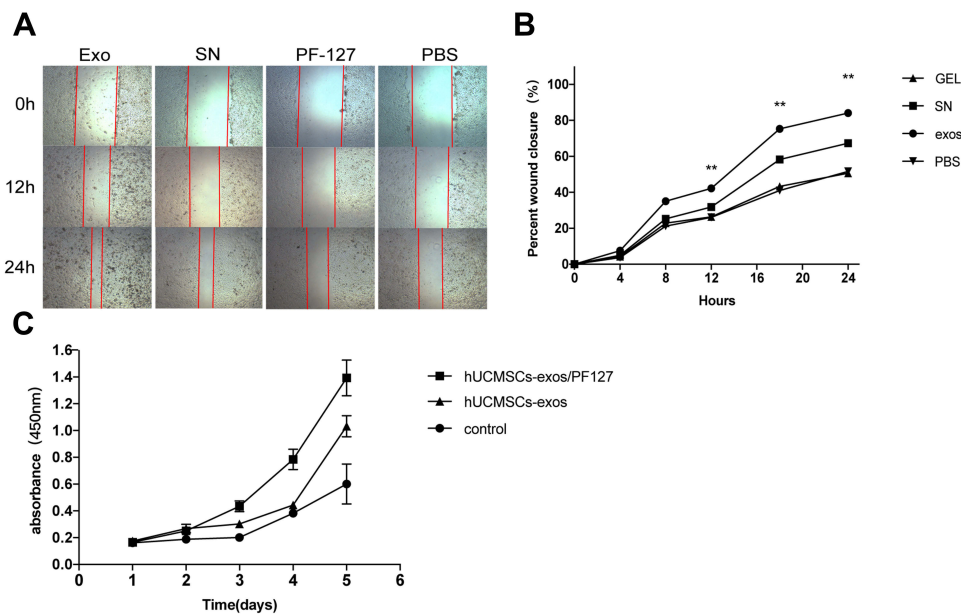


Figure 3 (A) Scratch test of human umbilical vein endothelial cell (HUVEC) and semiquantitative analysis. Exo, exosomes; SN, exosomes extraction supernatant; Gel, PF-127; control, PBS (phosphate-buffered saline). (B) Analyses of the wound closure. $**p < 0.01$. (C) CCK-8 assays of HUVEC proliferation.

General Conditions of the Diabetic Rats

Thirty SD rats were administered STZ via rapid intraperitoneal injection to generate a model of diabetes. A total of 4 rats died during the model-establishment process and the

induction success rate was 88.57%. The blood glucose levels of all the rats were above 16.67 mmol/L three days after injection and remained stable throughout the experiment. Rat weight, which was measured in all rats at set time points,

Table 2 Blood Glucose Levels and Weight of Experimental Rats (Mean±sd)

| | Before Injection (FBG*) | 3 Days After Injection (RBG#) | 1 Week After Injection (RBG) | 2 Weeks After Injection (RBG) | 3 Weeks After Injection (RBG) |
|------------------------------|-------------------------|-------------------------------|------------------------------|-------------------------------|-------------------------------|
| Blood glucose (mmol/L, n=26) | 4.15±0.3 | 25.90±3.0 | 26.78±2.5 | 25.79±3.7 | 26.29±3.2 |
| Weight (g, n=26) | 286.48±12 | 289.93±10 | 299.87±11 | 321.15±10 | 310.51±11 |

Notes: *FBG, fasting blood glucose; #RBG, random blood glucose.

Abbreviations: MSC-exos, mesenchymal stem cell-derived exosomes; PF-127, Pluronic F-127; hUCMSCs, human umbilical cord mesenchymal stem cell; hUCMSCs-exos, human umbilical cord mesenchymal stem cell-derived exosomes; HUVECs, human umbilical vein endothelial cell; VEGF, vascular endothelial growth factor; TGFβ-1, factor transforming growth factor beta-1; DFUs, diabetic foot ulcers; EVs, extracellular vesicles; miRNA, microRNA; hUCMSCs-exos/PF-127, hUCMSCs-exos and PF-127 composite; SD rats, Sprague-Dawley rats; STZ, Streptozotocin; RT-PCR, reverse transcription-polymerase chain reaction; H&E, hematoxylin and eosin; MVD, microvascular density; ANOVA, one-way analysis of variance; IGT, initial gelling temperature; AMSCs-exo, adipose-derived mesenchymal stem cells exosomes; ADSCs, adipose-derived stem cells; SEM, scanning electron microscopy; FBG, fasting blood glucose; RBG, random blood glucose; PBS, phosphate-buffered saline.

initially increased slowly and then showed negative growth three weeks after injection (Table 2). All the rats showed obvious symptoms of polydipsia, accompanied by polyuria, polyphagia and weight loss.

Wound Healing Rate

Full-thickness skin wounds on the backs of diabetic rats were created and treated with hUCMSC-exos/PF-127, hUCMSC-exos, PF-127 hydrogel or PBS. Representative images of wound area in each group at 0, 3, 7, 10 and 14 days after surgery are shown (Figure 4A). On day 3 after the operation, there was no significant differences in wound healing among the groups. However, the wound area was significantly smaller in the hUCMSC-exos/PF-127 group than in the other groups on days 7, 10 and 14 ($p<0.05$). This finding suggests that the hydrogel supports exosome survival and biological activity. On day 14, the wounds in the hUCMSC-exos/PF-127 group were almost completely healed, while the wound healing rates in the hUCMSC-exos, PF-127 hydrogel and

control groups were 8.95%, 14.52% and 23.09%, respectively (Figure 4B)

Histology

The histological structure of the regenerated dermis was analyzed on day 14. As shown in Figure 5, the epidermis of the new granulation tissue was intact and thick in all groups. However, in the hUCMSC-exos/PF-127 group, new hair follicle formation was evident in the center of the wound surface, fibroblasts were proliferating under the epidermis, and collagen deposition was sufficient and orderly. These phenomena were not observed in the hUCMSC-exos and PF-127 groups. No new hair follicles in the wound center were found in the control group or the PF-127 hydrogel group. In the control group, significant inflammatory cell infiltration was still observed at day 14.

Angiogenesis

Angiogenesis is pivotal throughout the entire process of wound repair. Blood vessels provide progenitor cells,

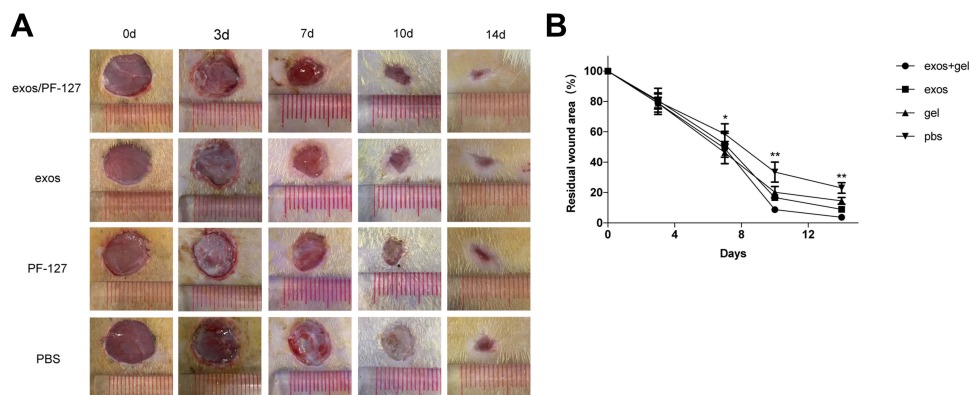


Figure 4 (A) Representative images of the wound surface in each group on days 0, 3, 7, 10 and 14. **(B)** Changes in the wound area over time. The following comparisons revealed significant differences ($*p<0.05$, $**p<0.01$): hUCMSC-exos/PF-127 group vs hUCMSC-exos, PF-127 hydrogel or control group. Exos/PF-127, exosomes combined with PF-127; exos, exosomes; gel, PF-127; control, PBS (phosphate-buffered saline).

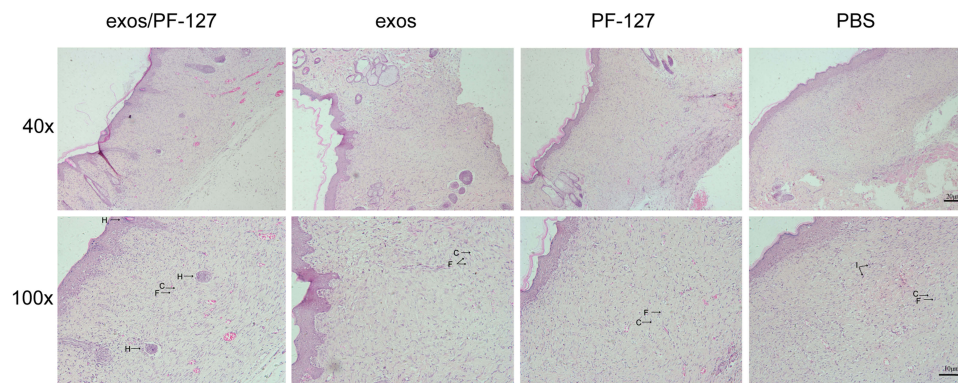


Figure 5 Histological analyses of Hematoxylin and eosin stained wounds on day 14 in the hUCMSC-exos/PF-127, hUCMSC-exos, PF-127 hydrogel and control groups. F, fibroblast, C, collagen, H, newly formed hair follicle; I, inflammatory cell. Exos/PF-127: exosomes combined with PF-127; exos, exosomes; gel, PF-127; control, PBS (phosphate-buffered saline).

oxygen and nutrients to maintain proliferation and remodeling at the wound site.²⁹ CD31 is an endothelial cell marker that can be used for immunohistochemical staining to confirm the degree of tissue vascularization. As shown in Figure 6A, the number of blood vessels was significantly higher in the hUCMSC-exos/PF-127 and hUCMSC-exos groups than in the PF-127 hydrogel or control group after 7 days of treatment. MVD density on day 14 was

significantly higher in the hUCMSC-exos/PF-127 and hUCMSC-exos groups than that in the other groups (Figure 6B, ** $p < 0.01$).

Ki67 Immunofluorescence

To identify the potential mechanism by which hUCMSC-exos/PF-127, hUCMSC-exos, PF-127 hydrogel and PBS affect cells in granulation tissue, we performed

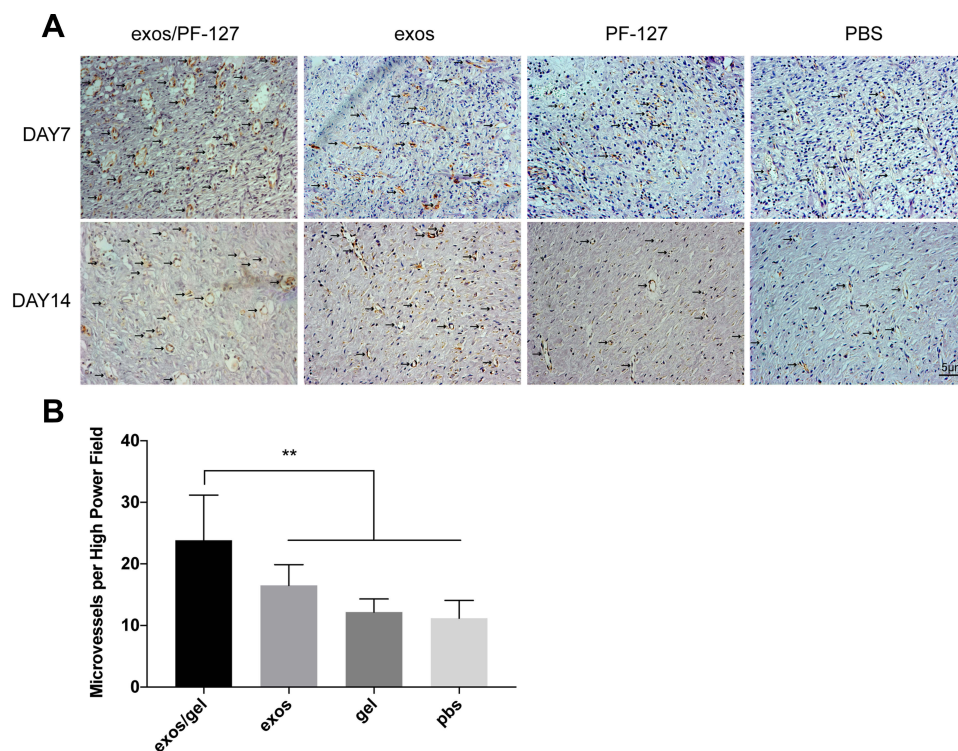


Figure 6 (A) Representative images of CD31 (vascular endothelial cell marker) immunohistochemistry on wound sections at days 7 and 14 from the hUCMSC-exos/PF-127, hUCMSC-exos, PF-127 hydrogel and control groups. Black arrows indicate microvessels in the wound tissues on day 14. **(B)** Analyses of microvessel densities of various treatment groups on day 14 (n=6). ** $p < 0.01$. Exos/PF-127, exosomes combined with PF-127; exos, exosomes; gel, PF-127; control, PBS (phosphate-buffered saline).

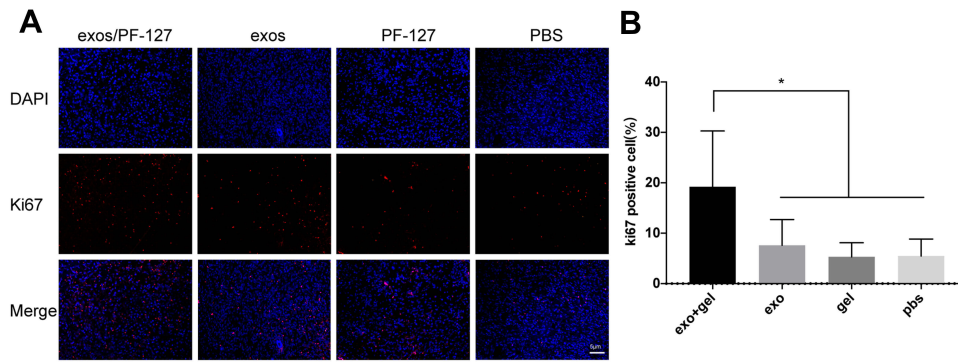


Figure 7 (A) Ki67 immunofluorescence to evaluate the effects of treatment on cell proliferation in the wounds. Immunofluorescence staining for Ki67 (red) and nuclear counterstaining with DAPI (blue, nucleus staining solution) on day 7 in the hUCMSC-exos/PF-127, hUCMSC-exos, PF-127 hydrogel and control groups. **(B)** Quantification analyses of Ki67-positive cells in the granulation tissues (n=6). *p<0.05. Exos/PF-127: exosomes combined with PF-127; exos, exosomes; gel, PF-127; control, PBS (phosphate-buffered saline).

immunofluorescence staining of Ki67, which is expressed by proliferating cells. On day 7 after wound generation, Ki67 was highly expressed in the hUCMSC-exos/PF-127 group, and a few positive cells were observed in the hUCMSC-exos, PF-127 hydrogel and PBS groups (Figure 7A and B, *p<0.05).

VEGF and TGFβ-I Expression Levels

RT-PCR was performed to investigate whether the two growth factors, VEGF and TGFβ-1, which have important effects on wound healing, were differentially expressed among the treatments. VEGF expression levels in granulation tissue were significantly higher in the hUCMSC-exos

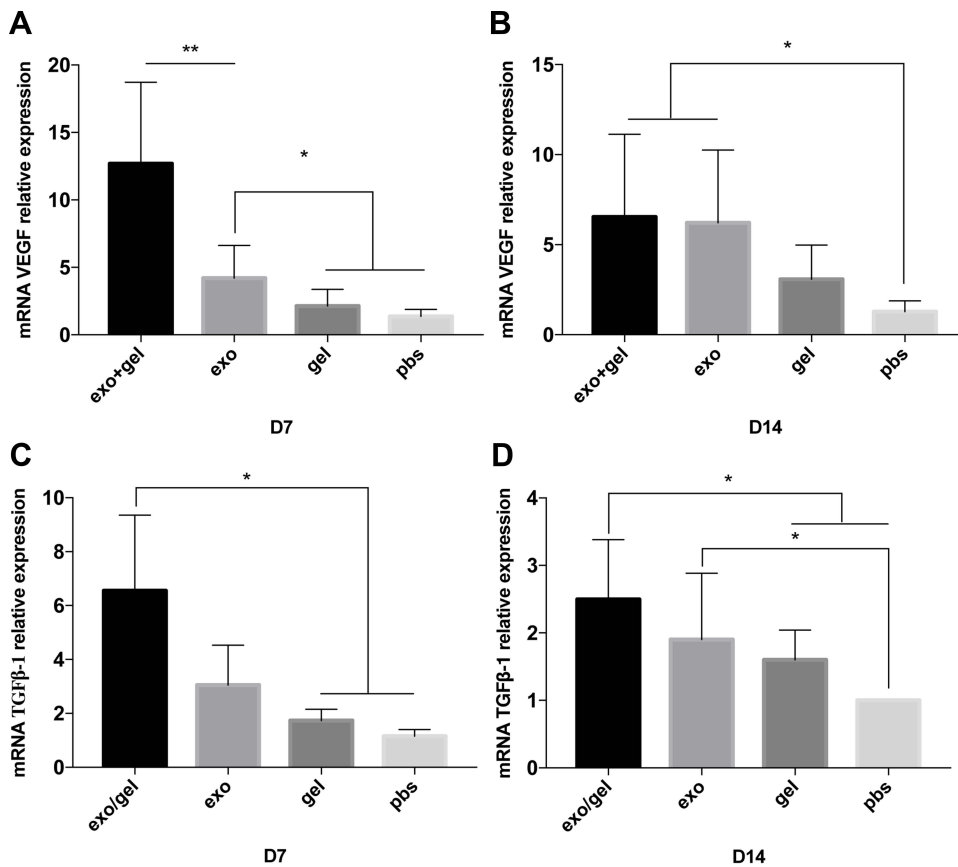


Figure 8 The relative mRNA expression levels of vascular endothelial growth factor (VEGF) (A and B) and transforming growth factor beta-1 (TGFβ-1) (C and D) on days 7 and 14 in wound tissue of the hUCMSC-exos/PF-127, hUCMSC-exos, PF-127 hydrogel and control groups. *p<0.05, **p<0.01. Exos/PF-127, exosomes combined with PF-127; exos, exosomes; gel, PF-127; control, PBS (phosphate-buffered saline).

/PF-127 and hUCMSC-exos groups than in the PF-127 hydrogel and control groups on days 7 and 14 (Figure 8A and B, ** $p < 0.01$). TGF β -1 expression levels in granulation tissue were significantly higher in the hUCMSC-exos/PF-127 and hUCMSC-exos groups than in the control group on days 7 and 14, but there was no significant difference between the PF-127 hydrogel and control groups (Figure 8C and D, * $p < 0.05$).

Discussion

Treatments based on hUCMSCs and certain cellular products can reduce the amputation rate and decrease the social and medical burdens of diabetes.^{30,31} In this study, we constructed a PF-127 and hUCMSC-exos composite and applied it to a diabetic rat cutaneous injury model to verify its ability to effectively prolong exosome survival in vitro. The PF-127 and hUCMSC-exos composite significantly promoted the healing of diabetic wounds, meanwhile, maintaining the bioactivity of hUCMSC-exos.

Many studies have focused on the stem cells therapies and biotechnologies of wound repair. Several kinds of stem cells, such as adipose-derived stem cells (ADSCs) and autologous growth factors have showed similar or distinct effects when applied to wounds. ADSCs and stromal vascular fraction (SVF) cells, which are heterogeneous cells that include ADSCs have been shown to support wound healing in human and animals wounds by promoting neo-angiogenesis and collagen synthesis and inducing a favorable immunomodulatory effect.³² ADSCs, which have multidirectional differentiation potential, have the ability to secrete exosomes containing microRNA, RNA and various of growth factors, inflammatory factors, cytokines and chemokines, including IL-6, IL-8 and TNF- α , which have anti-inflammatory effects and VEGF, which is involved in vascularization.^{33,34} Another type of stem cells, HFSCs, are similar to ADSCs in their ability to promote re-epithelization and improve angiogenesis and have the distinct property of promoting hair follicle regeneration.³⁵ HFSCs can migrate towards the injury site and then commit toward to terminally differentiated cells, participating in re-epithelialization and barrier repair.³⁶ Although the mechanism by which HFSCs promote wound healing remains unclear, evidence suggests that pathways including the Wnt, Bmp, Notch and Sonic hedgehog (SHH) pathways are involved in hair follicle regeneration and wound repair, among which the Wnt/ β -catenin pathway plays an important regulatory

role.^{37,38} Regarding the application of autologous growth factors, platelet-rich plasma (PRP) may be regarded as the representative which contains at least six major growth factors, including bFGF, PDGF, VEGF, EGF, TGF- β and IGF-1.³⁹ PRP can provide growth factors necessary for wound repair and regulate the dynamic balance between cells and extracellular matrix in the local microenvironment, providing favorable conditions for wound repair. For example, PDGF and VEGF could promote the proliferation, differentiation and angiogenesis of vascular endothelial cells.⁴⁰ TGF- β could lead to the apoptosis of inflammatory cells, control the degree of inflammatory response, boost keratinocyte proliferation and promote the deposition of extracellular matrix and the process of epithelialization.⁴¹ PRP also has a beneficial role in hair regrowth.⁴² In summary, the application of stem cells and PRP can aid wound repair by providing growth factors. In addition, stem cells can also secrete additional substances, such as exosomes and miRNA, to further promote wound repair.

Many basic and clinical studies have proven that hUCMSCs have desirable effects on chronic refractory wounds in patients with diabetes, including the stimulation of angiogenesis, the amelioration of diabetic peripheral neuropathy, and the regulation of immunity.^{30,31,43} The hUCMSCs used in this study were shown to promote wound healing and affect skin lesion repair by inducing β -catenin activation in endothelial cells and mediating angiogenesis through the delivery of 14-3-3 ζ , which induces YAP phosphorylation to influence wnt4 signaling pathways.^{20,27} Injection of hUCMSCs and CM has been found to increase the angiogenesis of wounds, possibly via the upregulated expression of PDGF and VEGF.⁴⁴ In addition, hUCMSCs also secrete miRNAs that reduce excessive scar hyperplasia and improve wound healing.⁴⁵ However, major application challenges, such as potential tumorigenicity, limited tissue targeting, frequent apoptosis and rapid clearance, and further research is needed.^{46,47} Recent studies have shown that stem cell-derived exosomes contain mRNAs, miRNAs, growth factors, and various other proteins that can participate in various physiological processes. These processes include hemostasis, thrombosis, inflammation, immune interactions, angiogenesis and processes in wound healing, such as re-epithelialization, neovascularization/blood vessel maturation, collagen deposition and development of hair follicles and sebaceous glands.^{18,48} For example, hUCMSC-exos containing miR-21, miR-23a, miR-125b, and miR-145 can inhibit fibroblast proliferation during wound healing to reduce scar

formation.⁴⁵ However, although exosomes have considerable medical prospects, their rapid expansion and inactivation at room temperature limit their applications.¹³

Previous studies have shown that a variety of hydrogels could promote the healing of chronic wounds. For example, a Poly-N-acetyl glucosamine hydrogel (matrix system) derived from microalgae shows a potential therapeutic effect though reducing exudates. Furthermore, wound cleaning could be achieved by the moisture content of the hydrogel.⁴⁹ PF-127 may have the similar efficacy mentioned above and has unique temperature-sensitive characteristics.⁵⁰ This biomaterial is liquid at low temperature and gradually solidifies as temperature increases, which means it can fit the irregular spaces of diabetic wounds. In the United States, PF-127, approved by the FDA for use in human, is widely used for drug delivery and controlled release due to its good biocompatibility and absorbability.⁵¹ A recent study used an injectable, self-healing and antibacterial polypeptide-based FHE hydrogel (F127/OHA-EPL) with the same thermo-responsive property as PF-127 in combination with adipose-derived mesenchymal stem cell exosomes (AMSCs-exos). The study revealed that the combination had the ability to stimulate the angiogenic response of HUVECs *in vitro* and neo-vascularization *in vivo* and showed great potential in promoting diabetic wound healing.⁵² We speculate that the PF-127 hydrogels can provide a moist environment for wound healing and act as a barrier against harmful substances, leading to the better healing performance in the PF-127 hydrogel group than in the control group.

Among the current methods of wound treatment and repair in diabetes, a proven MSC-exos-related method with good application prospects remains lacking. Our previous studies showed that PF-127 can encapsulate ADSCs, which then maintain a high survival rate and high biological activity of ADSCs within the material. Transplanting allogeneic ADSCs encapsulated by PF-127 onto wounds on diabetic rats effectively accelerated the wound healing rate and promoted cell proliferation and angiogenesis in granulation tissue.⁵³ Thus, to achieve improved performances through the combination of hydrogel and bioactive substances, we selected hUCMSC-exos in combination with PF-127 as a treatment for chronic diabetic wounds. We constructed a complex of PF-127 and hUCMSC-exos that maintained the biological activity of the exosomes and continuously released exosomes at the wound surface to promote wound healing. This is the first study to

investigate the efficacy of PF-127 hydrogel-encapsulated hUCMSC-exos to augment diabetic wound healing.

In this study, we cultured hUCMSCs and extracted exosomes from the cell supernatant with an exosome extraction kit. The extracted exosomes were verified to be at a high concentration and purity by scanning electron microscopy (SEM), NanoSight and Western blotting. Since the initial gelation temperature of PF-127 hydrogel decreases with increasing concentration, the initial gelation temperature and the time required to gel at 37°C were determined over a concentration gradient of 20%-28%. The results showed that 24% PF-127 had a moderate gel time and was therefore selected as the exosome carrier.

To investigate whether the extracted exosomes retained the ability to enter cells, we cocultured PKH67-labeled hUCMSC-exos with HUVECs. After 12 h of cocultivation, exosomes, indicated by green fluorescence, were observed in the cytoplasm, with localization and enrichment around the nucleus. When PBS and 24% PF-127 hydrogel were added to HUVECs as a control, no green fluorescence was observed. These findings suggest that extracted hUCMSC-exos can penetrate the cell membrane and concentrate around the nucleus, which may help them exert their functions. Considering that the duration of this assay was 12 h, we inferred that the PF-127 hydrogel extended exosome survival at room temperature compared with previous results.⁵⁴

Wound healing is a complex process involving various types of cells, including keratinocytes, endothelial cells, fibroblasts, platelets and macrophages, and various biochemical factors produced by these cells.⁵ Impaired angiogenesis is one of the most relevant factors delaying the healing of chronic diabetic wounds.^{55,56} Here, we intraperitoneally injected STZ into SD rats to induce type 1 diabetes mellitus and mimic impaired wound healing.

In this study, both hUCMSC-exos and hUCMSC-exos/PF-127 reduced the wound area in the first three days after treatment *in vivo*. Subsequently, hUCMSC-exos/PF-127 evoked a faster healing rate than the other treatments. We hypothesized that hUCMSC-exos play a significant role in the early stages of wound healing. However, exosomes are easily inactivated in the extracellular environment, leading to the failure of hUCMSC-exos to continuously produce biological effects in the wound during the intermediate and late stages of wound healing. In the hUCMSC-exos/PF-127 group, the biological activity of hUCMSC-exos was prolonged by the protection of the PF-127 gel, and we assume that these exosomes were

continuously released, leading to increased, sustained, and rapid wound healing.

To investigate the mechanisms underlying the effects of treatment on wound healing, we performed CD31 immunohistochemistry and quantified the MVD at injury sites on day 14. These data suggested that the hUCMSC-exos promoted angiogenesis in the hUCMSC-exos/PF-127 and hUCMSC-exos groups. Furthermore, compared with the hUCMSC-exos group, the hUCMSC-exos/PF-127 group showed increased angiogenesis, suggesting that greater numbers of functional exosomes might have been retained and continuously released during hydrogel-based delivery to the skin wound in the latter group.⁵² In vitro, a greater ability to promote HUVEC proliferation and migration was observed in the hUCMSC-exos/PF-127 group than that in the hUCMSC-exos group. Angiogenesis usually begins with endothelial cell proliferation and is followed by migration, adhesion, and differentiation.⁵⁷ Cell proliferation and migration are two key processes in angiogenesis and were found significantly increased in the hUCMSC-exos group. This finding suggests that the continuous release of functional exosomes by the composite could promote angiogenesis through accelerating endothelial cell proliferation and migration. In addition, VEGF mRNA expression levels were shown to have a similar increasing trend as the blood vessel density in the hUCMSC-exos/PF-127 and hUCMSC-exos groups. VEGF is an important factor that stimulates angiogenesis;⁵⁸ it binds at least two receptors that are mainly expressed on endothelial cells and synergizes with other angiogenic factors to stimulate and maintain the vascular system.⁵⁹ The reductions in VEGF and TGF β -1, which are thought to be associated with the decreased angiogenesis, may be the cause of delayed tissue healing in patients with diabetes.^{55,56} TGF β -1 is a growth factor that regulates a variety of cell functions, mainly cell growth and apoptosis, promotes the formation of granulation tissue by influencing fibroblast proliferation and differentiation and modifies the interaction between mural cells and endothelial cells.^{60,61} A recent study demonstrated that normalization of the M1/M2 macrophage ratio in granulation tissue, angiogenesis and tissue repair occurred in the dorsal wounds of STZ-induced type 1 diabetic mice that received a subcutaneous injection of recombinant mouse-derived TGF β -1.⁵⁵ In the hUCMSC-exos/PF-127 group, TGF β -1 mRNA expression levels were significantly increased compared with those in the PF-127 group and control group, while there was also an increasing trend of hUCMSC-exos group when compared with control group. A previous study showed that hUCMSC-

exos suppress excessive wound repair that leads to scarring by inhibiting TGF β -1,⁴⁵ and TGF β -1 has been shown to promote wound angiogenesis.⁶² Based on above observations regarding angiogenesis, we consider that the insignificant difference between the groups adding hUCMSC-exos and PF-127 was caused by the interaction between the two signaling pathways regulated by this factor.

On day 7, the number of actively proliferating Ki67-positive cells in the wound tissue was significantly increased in the hUCMSC-exos/PF-127 group compared with the other three groups. These results are consistent with the wound healing rate, angiogenesis and histological results, suggesting that the PF-127 hydrogel can serve as a scaffold to support exosomes, prolonging their survival in vitro and delivering them to diabetic wounds in situ. Thus, in situ hUCMSC-exos play an important role in diabetic wound healing by promoting cell proliferation and angiogenesis, and facilitating the formation of granulation tissue at the wound site.

In conclusion, the use of the complex may show enhanced survival of hUCMSC-exos in the inflammatory environment of a diabetic wound and retained hUCMSC-exos vitality. In this study, exosomes continued to act on wound tissue over time, promoting the vascularization of wound granulation tissue and ultimately shortening the diabetic wound healing time. The PF-127 hydrogel degrades rapidly in vivo and has no adverse effects on the host. This hydrogel enables the controlled release of various biochemicals and is an ideal biological scaffold for application in the complex environment of diabetic wounds and ulcers.

This study failed to elucidate the specific molecular mechanisms of angiogenesis after hUCMSC-exos transplantation in vivo. We need to clarify the further mechanisms by which hUCMSC-exos or other intervening exosomes could regulate angiogenesis. Many studies have shown that the role of exosomes mainly depends on the miRNA they contained. The use of different inventions to stimulate cells can regulate their secreted exosomes which may contribute to different effects on the target subjects. Yang et al showed that blue light exposure could elevated levels of miR-135b-5p and miR-499a-3p to increased proangiogenic capacity in MSC-exos.⁶³ Therapy based on photon energy has been broadly recommended as a method to accelerate diabetic wound healing. A future strategy for wound management might involve a noninvasive, economical, and multipurpose light-dependent cellular treatment.

Conclusion

In summary, we successfully constructed a composite of hUCMSC-exos and a PF-127 thermosensitive hydrogel for the treatment of chronic diabetic wounds. The PF-127 thermosensitive hydrogel is suitable for carrying and continuously releasing exosomes to promote angiogenesis by endothelial cells at the wound surface. Both in vivo and in vitro, the complexes maintained the biological activity of exosomes and promoted angiogenesis and cell proliferation. Upon the application of exosome-hydrogel composites, the wound healing rate accelerated, epithelial regeneration improved, and skin appendages showed better healing. This study shows that loading exosomes on biological scaffolds could enable the continuous release of exosomes and other biomolecules, stimulate early angiogenesis in diabetic wounds and promote wound healing and skin remodeling.

Acknowledgments

This work was supported by the Guangzhou Science and Technology Projects of China (grant number. 201604020007).

Disclosure

The authors report no conflicts of interest in this work.

References

1. Cho NH, Shaw JE, Karuranga S, et al. IDF diabetes atlas: global estimates of diabetes prevalence for 2017 and projections for 2045. *Diabetes Res Clin Pract.* 2018;138:271–281. doi:10.1016/j.diabres.2018.02.023
2. Liu C, Ge HM, Liu BH, et al. Targeting pericyte-endothelial cell crosstalk by circular RNA-cPWWP2A inhibition aggravates diabetes-induced microvascular dysfunction. *Proc Natl Acad Sci U S A.* 2019;116(15):7455–7464. doi:10.1073/pnas.1814874116
3. Frykberg RG, Zgonis T, Armstrong DG, et al. Diabetic foot disorders. A clinical practice guideline (2006 revision). *J Foot Ankle Surg.* 2006;45(5):S1–66. doi:10.1016/S1067-2516(07)60001-5
4. Singh N, Armstrong DG, Lipsky BA. Preventing foot ulcers in patients with diabetes. *JAMA.* 2005;293(2):217–228. doi:10.1001/jama.293.2.217
5. Davis FM, Kimball A, Boniakowski A, Gallagher K. Dysfunctional wound healing in diabetic foot ulcers: new crossroads. *Curr Diab Rep.* 2018;18(1):2. doi:10.1007/s11892-018-0970-z
6. Boulton AJ, Vileikyte L, Ragnarson-Tennvall G, Apelqvist J. The global burden of diabetic foot disease. *Lancet.* 2005;366(9498):1719–1724. doi:10.1016/S0140-6736(05)67698-2
7. Vijayakumar V, Samal SK, Mohanty S, Nayak SK. Recent advancements in biopolymer and metal nanoparticle-based materials in diabetic wound healing management. *Int J Biol Macromol.* 2019;122:137–148. doi:10.1016/j.ijbiomac.2018.10.120
8. Brem H, Tomic-Canic M. Cellular and molecular basis of wound healing in diabetes. *J Clin Invest.* 2007;117(5):1219–1222. doi:10.1172/JCI32169
9. Walter MN, Wright KT, Fuller HR, MacNeil S, Johnson WE. Mesenchymal stem cell-conditioned medium accelerates skin wound healing: an in vitro study of fibroblast and keratinocyte scratch assays. *Exp Cell Res.* 2010;316(7):1271–1281. doi:10.1016/j.yexcr.2010.02.026
10. Jeon YK, Jang YH, Yoo DR, Kim SN, Lee SK, Nam MJ. Mesenchymal stem cells' interaction with skin: wound-healing effect on fibroblast cells and skin tissue. *Wound Repair Regen.* 2010;18(6):655–661. doi:10.1111/j.1524-475X.2010.00636.x
11. Luo G, Cheng W, He W, et al. Promotion of cutaneous wound healing by local application of mesenchymal stem cells derived from human umbilical cord blood. *Wound Repair Regen.* 2010;18(5):506–513. doi:10.1111/j.1524-475X.2010.00616.x
12. Schlosser S, Dennler C, Schweizer R, et al. Paracrine effects of mesenchymal stem cells enhance vascular regeneration in ischemic murine skin. *Microvasc Res.* 2012;83(3):267–275. doi:10.1016/j.mvr.2012.02.011
13. Liu X, Yang Y, Li Y, et al. Integration of stem cell-derived exosomes with in situ hydrogel glue as a promising tissue patch for articular cartilage regeneration. *Nanoscale.* 2017;9(13):4430–4438. doi:10.1039/C7NR00352H
14. Gu J, Liu N, Yang X, Feng Z, Qi F. Adipose-derived stem cells seeded on PLCL/P123 electrospun nanofibrous scaffold enhance wound healing. *Biomed Mater.* 2014;9(3):035012. doi:10.1088/1748-6041/9/3/035012
15. Smith AN, Willis E, Chan VT, et al. Mesenchymal stem cells induce dermal fibroblast responses to injury. *Exp Cell Res.* 2010;316(1):48–54. doi:10.1016/j.yexcr.2009.08.001
16. Wagner J, Kean T, Young R, Dennis JE, Caplan AI. Optimizing mesenchymal stem cell-based therapeutics. *Curr Opin Biotechnol.* 2009;20(5):531–536. doi:10.1016/j.copbio.2009.08.009
17. Tong C, Hao H, Xia L, et al. Hypoxia pretreatment of bone marrow-derived mesenchymal stem cells seeded in a collagen-chitosan sponge scaffold promotes skin wound healing in diabetic rats with hindlimb ischemia. *Wound Repair Regen.* 2016;24(1):45–56. doi:10.1111/wrr.12369
18. Rackov G, Garcia-Romero N, Esteban-Rubio S, Carrion-Navarro J, Belda-Iniesta C, Ayuso-Sacido A. Vesicle-mediated control of cell function: the role of extracellular matrix and microenvironment. *Front Physiol.* 2018;9:651. doi:10.3389/fphys.2018.00651
19. Merino-Gonzalez C, Zuniga FA, Escudero C, et al. Mesenchymal stem cell-derived extracellular vesicles promote angiogenesis: potential clinical application. *Front Physiol.* 2016;7:24. doi:10.3389/fphys.2016.00024
20. Zhang B, Wu X, Zhang X, et al. Human umbilical cord mesenchymal stem cell exosomes enhance angiogenesis through the Wnt4/ β -catenin pathway. *Stem Cells Transl Med.* 2015;4(5):513–522. doi:10.5966/sctm.2014-0267
21. Zhang J, Guan J, Niu X, et al. Exosomes released from human induced pluripotent stem cells-derived MSCs facilitate cutaneous wound healing by promoting collagen synthesis and angiogenesis. *J Transl Med.* 2015;13(1):49. doi:10.1186/s12967-015-0417-0
22. Yap LS, Yang MC. Evaluation of hydrogel composing of Pluronic F127 and carboxymethyl hexanoyl chitosan as injectable scaffold for tissue engineering applications. *Colloids Surf B Biointerfaces.* 2016;146:204–211. doi:10.1016/j.colsurfb.2016.05.094
23. Shi Q, Qian Z, Liu D, et al. GMSC-derived exosomes combined with a chitosan/silk hydrogel sponge accelerates wound healing in a diabetic rat skin defect model. *Front Physiol.* 2017;8:904. doi:10.3389/fphys.2017.00904
24. Zhang K, Zhao X, Chen X, et al. Enhanced therapeutic effects of mesenchymal stem cell-derived exosomes with an injectable hydrogel for hindlimb ischemia treatment. *ACS Appl Mater Interfaces.* 2018;10(36):30081–30091. doi:10.1021/acsami.8b08449
25. Chen WJ, Huang JW, Niu CC, et al. Use of fluorescence labeled mesenchymal stem cells in pluronic F127 and porous hydroxyapatite as a bone substitute for posterolateral spinal fusion. *J Orthop Res.* 2009;27(12):1631–1636. doi:10.1002/jor.20925
26. Akash MS, Rehman K, Sun H, Chen S, Catapano A. Sustained delivery of IL-1Ra from PF127-gel reduces hyperglycemia in diabetic GK-rats. *PLoS One.* 2013;8(2):e55925. doi:10.1371/journal.pone.0055925

27. Zhang B, Wang M, Gong A, et al. HucMSC-exosome mediated-Wnt4 signaling is required for cutaneous wound healing. *Stem Cells*. 2015;33(7):2158–2168. doi:10.1002/stem.1771
28. Kant V, Gopal A, Kumar D, et al. Topical pluronic F-127 gel application enhances cutaneous wound healing in rats. *Acta Histochem*. 2014;116(1):5–13. doi:10.1016/j.acthis.2013.04.010
29. Okonkwo UA, DiPietro LA. Diabetes and wound angiogenesis. *Int J Mol Sci*. 2017;18(7):1419. doi:10.3390/ijms18071419
30. Zhou Y, Zhu Y, Zhang L, et al. Human stem cells overexpressing miR-21 promote angiogenesis in critical limb ischemia by targeting CHIP to enhance HIF-1 α activity. *Stem Cells*. 2016;34(4):924–934. doi:10.1002/stem.2321
31. Xia N, Xu JM, Zhao N, Zhao QS, Li M, Cheng ZF. Human mesenchymal stem cells improve the neurodegeneration of femoral nerve in a diabetic foot ulceration rats. *Neurosci Lett*. 2015;597:84–89. doi:10.1016/j.neulet.2015.04.038
32. Bi H, Li H, Zhang C, et al. Stromal vascular fraction promotes migration of fibroblasts and angiogenesis through regulation of extracellular matrix in the skin wound healing process. *Stem Cell Res Ther*. 2019;10(1):302. doi:10.1186/s13287-019-1415-6
33. Kilroy GE, Foster SJ, Wu X, et al. Cytokine profile of human adipose-derived stem cells: expression of angiogenic, hematopoietic, and pro-inflammatory factors. *J Cell Physiol*. 2007;212(3):702–709. doi:10.1002/jcp.21068
34. Atalay S, Coruh A, Deniz K. Stromal vascular fraction improves deep partial thickness burn wound healing. *Burns*. 2014;40(7):1375–1383. doi:10.1016/j.burns.2014.01.023
35. Liu F, Zhou H, Du W, et al. Hair follicle stem cells combined with human allogeneic acellular amniotic membrane for repair of full thickness skin defects in nude mice. *J Tissue Eng Regen Med*. 2020;14(5):723–735. doi:10.1002/term.3035
36. Ito M, Liu Y, Yang Z, et al. Stem cells in the hair follicle bulge contribute to wound repair but not to homeostasis of the epidermis. *Nat Med*. 2005;11(12):1351–1354. doi:10.1038/nm1328
37. Huang C, Du Y, Nabzdyk CS, et al. Regeneration of hair and other skin appendages: a microenvironment-centric view. *Wound Repair Regen*. 2016;24(5):759–766. doi:10.1111/wrr.12451
38. Tsai SY, Sennett R, Rezza A, et al. Wnt/ β -catenin signaling in dermal condensates is required for hair follicle formation. *Dev Biol*. 2014;385(2):179–188. doi:10.1016/j.ydbio.2013.11.023
39. Cervelli V, Scioli MG, Gentile P, et al. Platelet-rich plasma greatly potentiates insulin-induced adipogenic differentiation of human adipose-derived stem cells through a serine/threonine kinase Akt-dependent mechanism and promotes clinical fat graft maintenance. *Stem Cells Transl Med*. 2012;1(3):206–220. doi:10.5966/sctm.2011-0052
40. Langer H, May AE, Daub K, et al. Adherent platelets recruit and induce differentiation of murine embryonic endothelial progenitor cells to mature endothelial cells in vitro. *Circ Res*. 2006;98(2):e2–10. doi:10.1161/01.RES.0000201285.87524.9e
41. Chong DLW, Trinder S, Labelle M, et al. Platelet-derived transforming growth factor- β 1 promotes keratinocyte proliferation in cutaneous wound healing. *J Tissue Eng Regen Med*. 2020;14(4):645–649. doi:10.1002/term.3022
42. Gentile P, Garcovich S, Bielli A, Scioli MG, Orlandi A, Cervelli V. The effect of platelet-rich plasma in hair regrowth: a randomized placebo-controlled trial. *Stem Cells Transl Med*. 2015;4(11):1317–1323. doi:10.5966/sctm.2015-0107
43. Kuchroo P, Dave V, Vijayan A, Viswanathan C, Ghosh D. Paracrine factors secreted by umbilical cord-derived mesenchymal stem cells induce angiogenesis in vitro by a VEGF-independent pathway. *Stem Cells Dev*. 2015;24(4):437–450. doi:10.1089/scd.2014.0184
44. Shrestha C, Zhao L, Chen K, He H, Mo Z. Enhanced healing of diabetic wounds by subcutaneous administration of human umbilical cord derived stem cells and their conditioned media. *Int J Endocrinol*. 2013;2013:592454. doi:10.1155/2013/592454
45. Fang S, Xu C, Zhang Y, et al. Umbilical cord-derived mesenchymal stem cell-derived exosomal MicroRNAs suppress myofibroblast differentiation by inhibiting the transforming growth factor- β /SMAD2 pathway during wound healing. *Stem Cells Transl Med*. 2016;5(10):1425–1439. doi:10.5966/sctm.2015-0367
46. Lee PY, Cobain E, Huard J, Huang L. Thermosensitive hydrogel PEG-PLGA-PEG enhances engraftment of muscle-derived stem cells and promotes healing in diabetic wound. *Mol Ther*. 2007;15(6):1189–1194. doi:10.1038/sj.mt.6300156
47. Futrega K, King M, Lott WB, Doran MR. Treating the whole not the hole: necessary coupling of technologies for diabetic foot ulcer treatment. *Trends Mol Med*. 2014;20(3):137–142. doi:10.1016/j.molmed.2013.12.004
48. Wu P, Zhang B, Shi H, Qian H, Xu W. MSC-exosome: a novel cell-free therapy for cutaneous regeneration. *Cytotherapy*. 2018;20(3):291–301. doi:10.1016/j.jcyt.2017.11.002
49. Pietramaggiore G, Yang HJ, Scherer SS, et al. Effects of poly-N-acetyl glucosamine (pGlcNAc) patch on wound healing in db/db mouse. *J Trauma*. 2008;64(3):803–808. doi:10.1097/01.ta.0000244382.13937.a8
50. Almeida H, Amaral MH, Lobao P, Lobo JM. Pluronic[®] F-127 and pluronic lecithin organogel (PLO): main features and their applications in topical and transdermal administration of drugs. *J Pharm Pharm Sci*. 2012;15(4):592–605. doi:10.18433/J3HW2B
51. Diniz IM, Chen C, Xu X, et al. Pluronic F-127 hydrogel as a promising scaffold for encapsulation of dental-derived mesenchymal stem cells. *J Mater Sci Mater Med*. 2015;26(3):153. doi:10.1007/s10856-015-5493-4
52. Wang M, Wang C, Chen M, et al. Efficient angiogenesis-based diabetic wound healing/skin reconstruction through bioactive antibacterial adhesive ultraviolet shielding nanodressing with exosome release. *ACS Nano*. 2019;13(9):10279–10293. doi:10.1021/acsnano.9b03656
53. Kaisang L, Siyu W, Lijun F, Daoyan P, Xian CJ, Jie S. Adipose-derived stem cells seeded in Pluronic F-127 hydrogel promotes diabetic wound healing. *J Surg Res*. 2017;217:63–74. doi:10.1016/j.jss.2017.04.032
54. Jin Y, Chen K, Wang Z, et al. DNA in serum extracellular vesicles is stable under different storage conditions. *BMC Cancer*. 2016;16(1):753. doi:10.1186/s12885-016-2783-2
55. Okizaki S, Ito Y, Hosono K, et al. Suppressed recruitment of alternatively activated macrophages reduces TGF- β 1 and impairs wound healing in streptozotocin-induced diabetic mice. *Biomed Pharmacother*. 2015;70:317–325. doi:10.1016/j.biopha.2014.10.020
56. Galiano RD, Tepper OM, Pelo CR, et al. Topical vascular endothelial growth factor accelerates diabetic wound healing through increased angiogenesis and by mobilizing and recruiting bone marrow-derived cells. *Am J Pathol*. 2004;164(6):1935–1947. doi:10.1016/S0002-9440(10)63754-6
57. Daub JT, Merks RM. A cell-based model of extracellular-matrix-guided endothelial cell migration during angiogenesis. *Bull Math Biol*. 2013;75(8):1377–1399. doi:10.1007/s11538-013-9826-5
58. Zubair M, Ahmad J. Role of growth factors and cytokines in diabetic foot ulcer healing: a detailed review. *Rev Endocr Metab Disord*. 2019;20(2):207–217. doi:10.1007/s11154-019-09492-1
59. Carmeliet P. Mechanisms of angiogenesis and arteriogenesis. *Nat Med*. 2000;6(4):389–395. doi:10.1038/74651
60. Pastar I, Stojadinovic O, Krzyzanowska A, et al. Attenuation of the transforming growth factor β -signaling pathway in chronic venous ulcers. *Mol Med*. 2010;16(3–4):92–101. doi:10.2119/molmed.2009.00149

61. Lichtman MK, Otero-Vinas M, Falanga V. Transforming growth factor beta (TGF- β) isoforms in wound healing and fibrosis. *Wound Repair Regen.* 2016;24(2):215–222. doi:10.1111/wrr.12398
62. Yuan Y, Gao J, Liu L, Lu F. Role of adipose-derived stem cells in enhancing angiogenesis early after aspirated fat transplantation: induction or differentiation? *Cell Biol Int.* 2013;37(6):547–550. doi:10.1002/cbin.10068
63. Yang K, Li D, Wang M, et al. Exposure to blue light stimulates the proangiogenic capability of exosomes derived from human umbilical cord mesenchymal stem cells. *Stem Cell Res Ther.* 2019;10(1):358. doi:10.1186/s13287-019-1472-x

International Journal of Nanomedicine

Dovepress

Publish your work in this journal

The International Journal of Nanomedicine is an international, peer-reviewed journal focusing on the application of nanotechnology in diagnostics, therapeutics, and drug delivery systems throughout the biomedical field. This journal is indexed on PubMed Central, MedLine, CAS, SciSearch[®], Current Contents[®]/Clinical Medicine,

Journal Citation Reports/Science Edition, EMBase, Scopus and the Elsevier Bibliographic databases. The manuscript management system is completely online and includes a very quick and fair peer-review system, which is all easy to use. Visit <http://www.dovepress.com/testimonials.php> to read real quotes from published authors.

Submit your manuscript here: <https://www.dovepress.com/international-journal-of-nanomedicine-journal>